HHS Public Access

Author manuscript

Clin Neurophysiol. Author manuscript; available in PMC 2021 July 16.

Published in final edited form as:

Clin Neurophysiol. 2020 July ; 131(7): 1581–1588. doi:10.1016/j.clinph.2020.04.008.

Measuring conduction velocity distributions in peripheral nerves using neurophysiological techniques

Zhen Ni[a], **Felipe Vial**[a,b], **Alexandru V. Avram**[c], **Giorgio Leodori**[d], **Sinisa Pajevic**[e], **Peter J. Basser**[f,*], **Mark Hallett**[a,*]

[a]Human Motor Control Section, National Institute of Neurological Disorders and Stroke, National Institutes of Health

[b]Facultad de Medicina Clinica Alemana Universidad del Desarrollo, Santiago, Chile

[c]National Institute of Biomedical Imaging and Bioengineering, National Institutes of Health

[d]IRCCS Neuromed, Pozzilli, Italy

[e]Mathematical and Statistical Computing Laboratory, Center for Information Technology, National Institutes of Health

[f]Section on Quantitative Imaging and Tissue Sciences, *Eunice Kennedy Shriver* National Institute of Child Health and Human Development, National Institutes of Health

Abstract

Objective: To determine how long it takes for neural impulses to travel along peripheral nerve fibers in living humans.

Methods: A collision test was performed to measure the conduction velocity distribution of the ulnar nerve. Two stimuli at the distal and proximal sites were used to produce the collision. Compound muscle or nerve action potentials were recorded to perform the measurements on the motor or mixed nerve, respectively. Interstimulus interval was set at 1–5 ms. A quadri-pulse technique was used to measure the refractory period and calibrate the conduction time.

Results: Compound muscle action potential produced by the proximal stimulation started to emerge at the interstimulus interval of about 1.5 ms and increased with the increment in interstimulus interval. Two groups of motor nerve fibers with different conduction velocities were identified. The mixed nerve showed a wider conduction velocity distribution with identification of more subgroups of nerve fibers than the motor nerve.

Conclusions: The conduction velocity distributions in high resolution on a peripheral motor and mixed nerve are different and this can be measured with the collision test.

[*]**Address correspondence to: Mark Hallett, M.D.**, Chief, Human Motor Control Section, NINDS, NIH, Building 10, Room 7D37, 10 Center Dr. MSC 1428, Bethesda, MD 20892-1428, Tel: 301-496-9526, Fax: 301-480-2286, hallettm@ninds.nih.gov, and, **Peter J. Basser, Ph.D.**, Head, Section on Quantitative Imaging and Tissue Sciences, NICHD, National Institutes of Health (NIH), 13 South Drive, MSC 5772, Bldg. 13, Rm. 3W16, Bethesda, MD 20892-5772, Tel: 301-435-1949, Fax: 301-480-0163, basserp@helix.nih.gov.

Conflict of Interest Statement

None of the authors have potential conflicts of interest to be disclosed.

Significance: We provided ground truth data to verify the neuroimaging pipelines for the measurements of latency connectome in the peripheral nervous system.

Keywords

Collision; compound muscle action potential; compound nerve action potential; conduction velocity; motor nerve and mixed nerve; peripheral electrical nerve stimulation

1. Introduction

A nerve fiber is the slender and long projection of a neuron. Functionally, one neuron transmits information to muscles and other neurons through the electrical impulses on the nerve fiber (Debanne, 2004). Nerve fibers vary considerably in diameter (Hursh, 1939; Sherman and Brophy, 2005; Tomasi, et al., 2012). The conduction time between two nodes on a given nerve fiber are determined by the diameter of the fiber (Aminoff, 2012; Hartline and Colman, 2007). Recent advances in histological techniques validated the diameter measurements at the postmortem examination in human (Innocenti, et al., 2019; Innocenti, et al., 2014; Tomasi, et al., 2012). However, quantification of the distribution of nerve fiber diameters in a living human with a high resolution similar to that used in the postmortem examination has not been done. Therefore, in the current world of the cortical connectome (Oh, et al., 2014; Wedeen, et al., 2012), there is a need to develop an experimental pipeline for conduction latency distribution mapping (latency connectome) with high resolution (Fields, et al., 2015). The new framework will reveal how different neural elements are temporally connected via nerve fibers at millimeter spatial resolution and at millisecond time scale and will fill a knowledge gap between neuroscience research and the preclinical and clinical neuroimaging applications.

Histological analysis using electron microscopy can measure the nerve fiber diameters and the distribution of the diameters correctly in some areas in primates (Tomasi, et al., 2012). However, the invasive nature of the technique with biopsy and other technical problems including tissue preparation with section obtained from a limited area make the wide use of *in vivo* histological analysis infeasible for a living human (Gabriel, et al., 2000; Jacobs and Love, 1985). Our group has previously developed neuroimaging techniques using the non-Gaussian diffusion model based on q-space nuclear magnetic resonance concepts (Callaghan, et al., 1991), providing estimates of the average axon diameter and axon diameter distribution in the central and peripheral nervous systems (Assaf, et al., 2008; Avram, et al., 2016; Basser, et al., 2000; Komlosh, et al., 2013). While our previous works have addressed the possible sensitivity and accuracy of these techniques, measurements using neurophysiological and magnetic resonance imaging based predictions of nerve fiber morphology should be compared directly to open up a new window on studying the neuronal network functions. The conduction velocity distributions of a nerve bundle in a peripheral nerve with high resolution may be measured with a well-designed electrophysiological paradigm using a collision technique. Two electrical stimuli with changes in interstimulus interval at 0.1 ms step can be used to perform the functional measurements with a high temporal resolution. Therefore, we performed a proof-of-principle study to test the changes in compound muscle action potential with different stimulus intervals between the two

stimuli caused by different groups of nerve fibers with various conduction velocities. Our experiments are based on the selective re-stimulation of the faster fibers in the nerve bundle with a test stimulus applied to one site by blocking the slower fibers with a conditioning stimulus applied to a different site (Hopf, 1963; Ingram, et al., 1987b). Our purpose was to transform the physiological measurements into anatomical measurements in a peripheral nerve and use the data to vet and possibly validate the neuroimaging pipeline. In addition, the impulses in the afferent nerve fibers for certain sensory neurons travel from the periphery to the body of the neurons (Blagburn and Bacon, 2004). The peripheral nerve bundle is composed of both sensory and motor nerve fibers. It is well known that the diameter distributions of motor fibers and sensory fibers are different in a mixed nerve (Gesslbauer, et al., 2017). Therefore, we also measured the changes in compound nerve action potential recorded on a mixed nerve to determine whether there are different conduction velocity distributions of the whole peripheral nerve bundle with both motor and sensory nerve fibers. We hypothesized that nerve fibers with different diameters contribute differently to the compound muscle and nerve action potentials in the collision test. The distribution of nerve conduction velocities can be determined by measuring the cumulative contributions of different fibers in the compound action potentials.

2. Methods

2.1. Subjects

We studied 10 right-handed healthy subjects. All subjects provided written informed consent, and the clinical protocol (Clinicaltrials.gov Identifier NCT03223636) was approved by the Combined NeuroScience Institutional Review Board at the National Institutes of Health.

2.2. Experiment 1: Motor nerve test

The conduction velocity distribution on a motor nerve were measured using a collision test (Figure 1A). Compound muscle action potentials were recorded from the right abductor digit minimi muscle. Surface electromyograms were recorded using adhesive disposable surface electrodes (9013L0203, Alpine Biomed APS, Skovlunde, Denmark) with a shielded cable (HUSH™, 9013C0122) and a DIN connector. The electrodes, with small recording area (7 4 mm) and touch-proof connectors, provided highly accurate recordings and largely reduced the occurrence of double peaks which were common in the compound muscle action potential recordings. The active electrode was placed over the muscle belly, and the reference electrode over the metacarpophalangeal joint of the little finger. The distance between the two electrodes was about 2–3 cm. The signal was amplified (1000×), band-pass filtered (20 Hz-2.5 kHz, Neuropack MEB-2300 EMG/NCV/EP Measuring Desktop System, Nihon Kohden, Tokyo, Japan), and digitized at 5 kHz by an analog-to-digital interface (Micro1401, Cambridge Electronics Design, Cambridge, UK). The digitalized data were stored in a computer for off-line analysis. The right ulnar nerve was stimulated with electrical stimulations at a supramaximal intensity both at a proximal and distal site. The supramaximal intensity was 20% beyond the stimulus intensity needed to produce maximal compound muscle action potentials. The intensities for proximal and distal stimuli were determined separately. The distal conditioning stimulation (ulnar nerve at wrist, 0.1 ms

duration, 25.5 ± 7.6 mA) was given first and generated both an orthodromic (produced the first compound muscle action potential) and antidromic action potential on the nerve. The second proximal stimulation (forearm, 0.1 ms duration, 32.5 ± 7.2 mA) after an interstimulus interval collided with the antidromic action potential generated by the first distal stimulation. The later action potential produced by the proximal stimulation was the test response and it was blocked by the distal conditioning stimulation if the interval was short. As the nerve bundle is composed of multiple nerve fibers with different conduction velocities, progressively increasing the interstimulus interval allowed the antidromic action potential generated by the first distal stimulation to pass the site of second proximal stimulation on the nerve fibers with faster conduction (Figure 1B). This led to the gradual increase in the late (second) test compound muscle action potential (evoked by the orthodromic action potential generated by the proximal stimulation). Theoretically, sites of collision on nerve fibers with different conduction velocities are well separated if the distance between two stimuli is long. However, high stimulus intensity was required when the second proximal stimulation was moved close to the elbow due to the deeper location of ulnar nerve. In addition, we recorded compound nerve action potentials in Experiment 3 (see methods below). The stimulation close to elbow produced a large artifact which made the measurements less reliable. Eventually, the second proximal stimulation was given on the forearm (about 10 cm away from the cubital tunnel) and the distance between the sites of two stimuli was 9.6 ± 1.1 cm. We set the interstimulus intervals at 1–5 ms with an increment of 0.1 ms. Ideally, these intervals could verify the conduction velocity distribution measurement covering the range of about 20–100 m/s. The experimental configuration consisted of 41 states (experimental conditions) with different interstimulus intervals and 4 states for distal or proximal stimulus alone (2 states for each). Five trials for each experimental state (225 trials in total) were delivered in a random order. Stimulations were delivered with external triggers preprogrammed with an analog-to-digital interface (Micro1401, Cambridge Electronics Design, Cambridge, UK). The interval between two successive trials was set at 0.9–1.1 s. The skin temperature between two stimuli was 35.6 ± 0.7 ºC.

2.3. Experiment 2: Evaluation of refractory period

A technical issue related to the refractory period affects the accuracy of conduction velocity estimates obtained in the collision test. We used a quadri-pulse technique to measure the refractory period of the motor nerve (Figure 2). Two pulses with supramaximal intensity were given at both the distal and proximal sites. The interstimulus interval between two stimuli at the proximal site was fixed at 4 ms to avoid any potential interactions between the two impulses from the proximal site. The first pulse at the distal site and the first pulse at the proximal site were given simultaneously to ensure the first collision on all nerve fibers being tested. If the second pulse at the distal site were given without a time delay it would fall in the refractory period of the first pulse at the distal site and would not affect the orthodromic action potential produced by the second pulse at the proximal site (test pulse). With the increase in interstimulus interval between the two stimuli at the distal site, the second pulse can escape from the refractory period of the first pulse at the distal site and collide with the orthodromic action potential produced by the second pulse at the proximal site. The second collision on the nerve reduces the late (second) test compound muscle action potential

produced by the second pulse at the proximal site. We set the interstimulus interval between two distal stimuli at 0–2 ms with increment of 0.1 ms to cover the entire range of refractory periods. In addition to the second collision, the waveforms of the second pulse on the distal and proximal sites may also interact. We recorded trials for paired-pulse condition with two pulses on the distal site for each interstimulus interval and subtracted the paired-pulse trial from the quadri-pulse trial to remove their waveform interaction if necessary. We also recorded trials for a single-pulse both at the distal and proximal site and trials for a triple-pulse condition without the second pulse at the distal site. Therefore, the experimental configuration consisted of 22 states for both quadri-pulse and paired-pulse trials with different interstimulus intervals, and 6 states for distal or proximal stimulus alone or triple-pulse stimulus (2 states for each). Five trials for each experimental state (250 trials in total) were delivered in a random order.

2.4. Experiment 3: Mixed nerve test

The peripheral nerve bundle is composed of both sensory and motor nerve fibers and the motor nerve fibers may be a minority of fibers in a mixed nerve (Gesslbauer, et al., 2017). As the conduction velocity distributions on the sensory nerve and motor nerve may be different, we performed the collision test on the mixed ulnar nerve (Figure 3A). The experimental procedure was similar to that used for the measurement on the motor nerve. Importantly, the order of two stimuli used in the motor nerve test was reversed. Namely, the proximal stimulus on the forearm was applied at first as the conditioning stimulus. The distal stimulus on the wrist was applied later and produced a test response. Ten trials for each experimental state (41 states for different interstimulus intervals and 2 states for each distal or proximal stimulus alone, 450 trials in total) were delivered in a random order. The compound nerve action potentials which included signals with both sensory and motor components were recorded from the mixed ulnar nerve using the same surface electromyographic system as that used in the motor nerve test. The active electrode was placed at the epicondylar groove (slightly distal to the medial epicondyle of the elbow). The reference electrode was placed above the elbow. The distance between two recording electrodes was about 2–3 cm. We maintained the electrode-skin impedance below 5 kΩ to increase the sensitivity for the recording. The signal amplifier was set at a high gain (10,000×).

2.5. Data analysis

The amplitude of compound muscle or nerve potential was measured peak-to-peak. Changes in the test response (second compound muscle or nerve action potential) caused by preceding pulses were measured. The proportions of nerve fibers in the whole nerve bundle with certain conduction velocities were calculated. The proportion for a group of nerve fibers was represented by the percentage of the difference in compound muscle or nerve action potential with the minimal increase in interstimulus interval (0.1 ms) divided by the maximal compound muscle or nerve action potential. Conduction velocity was calculated by dividing the distance between two stimulus sites by the interstimulus interval (corrected by the refractory period). We used the median value of the refractory period measured in the quadri-pulse technique to calibrate the interstimulus interval measurement. The median value for refractory period was the interstimulus interval between two pulses at the distal site

used in the quadri-pulse experiment, which showed the maximal change in the test response within a 0.1 ms increment. The conduction velocity distribution was represented by the relationship between the proportion of nerve fibers and corresponding conduction velocity. In addition, the conduction velocities correspondence to the fastest 5%, slowest 5% and the largest (peak) proportion of fibers were identified.

3. Results

We studied 10 right-handed (Edinburgh Handedness Inventory, 94.0 ± 13.5) subjects (mean age of all subjects 29.7 ± 14.0 years, 4 women and 6 men).

3.1. Experiment 1: Motor nerve test

We performed collision tests on the motor nerve. Figure 1B and 1C showed that compound muscle action potential produced by the proximal stimulation started to emerge at the interstimulus interval of about 1.5 ms. The potential increased with the increment in interstimulus interval and reached a maximum at the interstimulus interval of about 4 ms. It should be mentioned that the compound muscle action potentials produced by the distal (conditioning) and proximal (test) stimuli interfered because the distance between two stimuli was short in the present study. We performed a waveform subtraction of recordings with distal stimulus alone from those with paired-pulse stimulus (Supplementary Figure S1). The proximal waveform after subtraction was slightly different from that before subtraction. In particular, the waveform after subtraction showed a small but early potential which did not appear in the recordings for proximal stimulus alone, likely due to the interference between the two stimuli. It arises from summation of the later component of the distal stimulus with the early component of the proximal stimulus. In addition, different stimulus artifacts under two experimental conditions could also have minor influence on the waveform subtraction. Importantly, the amplitudes of the test action potentials after waveform subtraction were similar to the amplitudes before subtraction. We found that there were two steps of increased amplitude of the test compound muscle action potential in most subjects, indicating two major components (subgroups) of fibers with different conduction velocities (Figure 1C and Table 1).

3.2. Experiment 2: Evaluation of refractory period

The refractory period on the ulnar nerve was measured with the quadri-pulse paradigm (Figure 2A). The first pulse at the distal site and proximal site produced the first collision. The second pulse at the distal site started to escape from the refractory period of the first pulse delivered at the same distal site at an interstimulus interval of about 0.8 ms and reduced the second (test) compound muscle action potential produced by the second pulse at the proximal site. The test compound muscle action potential disappeared at the interval of about 1.3 ms, indicating the end of refractory period of all fibers. The median value of the refractory period used for further data analysis was 1.12 ± 0.17 ms (Figure 2B and 2C).

3.3. Experiment 3: Mixed nerve test

Figure 3 showed that the result with the collision test on a mixed nerve was similar to that on a motor nerve. However, the compound nerve action potential produced by the distal test

stimulation started to emerge at the interstimulus interval of about 1.2 ms (slightly earlier than motor nerve) and reached a maximum at the interval of about 4.5 ms (later than the motor nerve). The amplitude increased with more steps in most subjects (Figure 3B and Table 1).

3.4. Conduction velocity distribution

Figure 4 confirmed two components with different peak proportions of the conduction velocity distribution curve for motor nerve. On the other hand, three peaks with less predominant proportion were found for the mixed nerve. Table 1 confirmed the similar results in most subjects. In addition, mixed nerve had wider conduction velocity distribution (at both the fast and slow end) than the motor nerve alone.

4. Discussion

Using the proposed collision test, we clearly identified the distribution of peripheral nerve fibers with different conduction velocities. This was the first study that investigated the conduction velocity distribution of a mixed nerve with a neurophysiological approach. Importantly, we found two peaks with different velocities at about 50 m/s and 90 m/s of the motor nerve. The conduction velocity distribution on the mixed nerve was wider than that of the motor nerve with more peaks.

4.1. Measurements on the motor nerve

The action potential propagation on a nerve fiber mediated by electrical current is much slower than other electrical currents flowing outside human body in the nature. However, the saltatory nerve conduction via action potential propagation is the fastest type of conduction in the human body mediated by biological current flows (Debanne, 2004). The relation between the diameter of a nerve fiber and conduction velocity of action potential is one of the strongest anatomical and functional relations in neurophysiology and neuroscience (Hartline and Colman, 2007; Hursh, 1939). As we used compound muscle action potential to measure the conduction velocity distribution on a motor nerve in the collision test, group A nerve fibers connecting alpha motoneurons and extrafusal muscle fibers are likely the main target of the distribution measurements on the motor nerve (Dumitru, 2000). The conduction velocity distribution of the motor fibers in a nerve was measured in early studies (Hopf, 1963; Ingram, et al., 1987b). Similar measurements were also performed with a single fiber electromyogram technique using a needle electrode (Padua, et al., 2007). However, a major confounding factor is that the first distal stimulation produced a refractory period on the nerve fibers after the action potential (Hartline and Colman, 2007; Hodgkin and Huxley, 1952; Tasaki, 1953) and the refractory period is inversely correlated to the diameter of the nerve fiber (Borg, 1980; Ingram, et al., 1987a). In addition, the shape of nerve fiber is not constant along the whole length and the relationship between compound muscle action potential and diameter of nerve fiber at the proximal stimulation site may be different from that at the distal stimulation site (Hartline and Colman, 2007; Hodgkin and Huxley, 1939; Hodgkin and Huxley, 1952). Therefore, the subnormal membrane potentials caused by post-activation excitability change on nerve fibers with different diameters or even at different sites on the same nerve fiber may be different. In this regard, the smaller compound muscle

action potential with the proximal stimulus compared to that with the distal stimulus is expected due to dispersion of action potentials on the nerve fibers (Olney, et al., 1987; Schulte-Mattler, et al., 2001). Another technical problem affecting the accuracy of our distribution measurements and previous studies with physiological techniques is that the recovery of membrane potential required a delay (refractory period) for the proximal test stimulation to overcome the antidromic current produced by the distal stimulation. We performed a quadri-pulse experiment to evaluate the refractory period (Ingram, et al., 1987a). It should be mentioned that the propagating impulses in an orthodromic direction generated by the proximal test stimulation was affected by the refractory period in the motor nerve test. On the other hand, we used the refractory period measured in the opposite (antidromic) direction obtained from the quadri-pulse experiment to calibrate the period for the motor nerve test. Although the difference in refractory periods with orthodromic and antidromic currents on the nerve fibers might lead to slight bias in the calculation of conduction velocity, our result after calibration of the refractory period that one component of the motor nerve fibers in the nerve bundle had a conduction velocity close to 100 m/s was consistent with the fastest conduction velocity of group A fibers estimated indirectly by electron microscopy (King, 2013; King and Ginsberg, 2013) and supported the classical model of the strong relationship between physiology and functional anatomy. However, it should be mentioned that similar conduction velocities compared to the previous studies with neurophysiological techniques (Hopf, 1963; Ingram, et al., 1987b) would be obtained if no correction for the refractory period was performed. The increased value of velocity after correction was predominant for the fastest fibers in the nerve bundle because the proportion of refractory period in the conduction time (reflected by the interstimulus interval) was the largest for the fastest fibers and the correction caused the greatest reduction in denominator for the calculation of velocity. Additionally, the distance between the two stimuli in our study was shorter than that in the previous studies (Hopf, 1963; Ingram, et al., 1987b). Therefore, the proportion of refractory period in the conduction time was further increased for the short distance between two stimuli. It may also be explained that the distal conditioning stimulation produced an absolute refractory period followed by a relative refractory period with subnormal membrane potential (Hodgkin and Huxley, 1939; Hodgkin and Huxley, 1952). A test stimulation applied after a short interstimulus interval with supramaximal intensity (20% above that produced maximal compound muscle action potential) likely overcomes the relative refractory period and shifts the conduction velocity distribution curve to the right side (with high velocity values). The distribution measurement may be further complicated by the subnormal membrane potential during the relative refractory period as it affects the conditioning and test stimulations differently. Moreover, studies performed in cats have demonstrated that the innervation ratio for motor nerve fibers with fast conduction velocity is larger than those with slow conduction velocity (Burke, et al., 1973; Burke and Tsairis, 1973). Therefore, the contribution of fast conducting fibers to the compound muscle action potential is likely more than that of the slow conducting fibers, potentially also shifting the distribution curve to the right side. Another important factor is that a virtual cathode could be induced just proximal to the anode with the first distal stimulus at a supramaximal intensity, making the virtual distance (between virtual cathode and anode) shorter than the distance between two physical electrodes. Collision might have occurred at shorter interstimulus interval, leading to a large value of conduction velocity. It

has been reported that rotating the anode slightly away from the nerve may remove the virtual cathode (Cummins, et al., 1979) and future experiments with such an arrangement may avoid the problem. Additionally, it was reported that decrease in temperature of a nerve segment reduces the conduction velocity while decrease in local temperature increases the compound muscle action potential amplitude (Ricker, et al., 1977; Stalberg, et al., 2019). We warmed the whole forearm and maintained the skin temperature between two stimuli but did not measure the skin temperature around the recording electrodes. Our result should not be affected by the factor of temperature.

Importantly, our collision test with high temporal resolution first identified two subgroups of fibers with different conduction velocities for the group A motor fibers (Figure 1C and Table 1). The conduction velocity of most fibers in the second subgroup was about 50 m/s after the correction due to the refractory period—at the low end of conduction velocities in group A motor fibers. It has long been argued that action potentials following closely behind a previously propagated impulse conduct more slowly for the first few centimeters (Tasaki, 1953). The short distance (less than 10 cm) was selected for setting up the two stimulating electrodes in our study to ensure a reliable maximal compound muscle action potential with both the distal and proximal stimulations. The delayed impulse may be more predominant on nerve fibers with slower conduction velocity, causing longer refractory periods on slower fibers (discussed above). Therefore, our calibration with a constant value of refractory period (median value measured with the quadri-pulse technique) for all fibers might be an underestimate of time in the slower fibers due to the inverse correlation between the refractory period and conduction velocity (Hartline and Colman, 2007). Another technical problem is that multiple peaks in the compound muscle action potential are common with quadri-pulse stimulation. Previous studies also reported similar waveforms with double peaks induced by a single conditioning and/or test stimulus alone (Ingram, et al., 1987a; Ingram, et al., 1987b). Summation of neural signals induced by different pulses made the interpretation of waveforms complex. Our recording system with advanced technology and short distance between active and reference electrodes (about 2–3 cm) largely reduced the occurrence of double peaks with a single-pulse stimulus. However, the complexity of waveform of compound muscle action potential recorded in the hypothenar muscles (abductor digiti minimi muscle in the present study)(van Dijk, et al., 1999) might still be a major confounding factor. Volume conduction from the interosseous muscles (McGill and Lateva, 1999) often produces double peaks in the reference electrode. Therefore, the signals recorded in the active and reference electrodes with a bipolar setting may be different in shape with influences from separate groups of muscles and nerve fibers. The different distortions of compound muscle action potential in the active and reference electrodes may be magnified by the slightly different distances of the two electrodes from the innervating nerve fibers and the interpretation of action potential after offline waveform subtraction was difficult. In addition, errors arising from transient changes in conduction may also occur in the target muscle due to the preceding maximal contraction produced by the first distal stimulation (Stalberg, 1966; Stalberg and Trontelj, 1997). Although our high-pass filter helped remove these errors and the stimulus artifact, signals with low frequency components might be lost. Similarly, our low-pass filter and sampling rate (only 2 times of the low-pass filter) might have lowered the amplitude and prolonged the main peaks of compound muscle

action potential. A higher sampling rate would be more suitable for the selected low-pass filter (Stalberg, et al., 2019; Tankisi, et al., 2020).

4.2. Measurements on the mixed nerve

The present study first measured the conduction velocity distribution in a mixed nerve with a well-designed experimental paradigm and with the anatomical accessibility provided by the superficial nature of ulnar nerve at the medial epicondyle of elbow. The peripheral nerve bundle is composed of myelinated group A and B fibers and unmyelinated group C fibers, which correspond to functional properties ranging from motor fibers to sensory fibers with various afferent inputs. The complex composition of mixed nerve is also supported by recent histological findings that the proportion of motor fibers in the upper limb nerve is extremely low (Gesslbauer, et al., 2017). Therefore, it is not surprising that the mixed nerve had a wider conduction velocity distribution than the motor nerve alone and more subgroups of nerve fibers with different peak conduction velocities were distinguished in the mixed nerve bundle in our study (Figure 4 and Table 1). However, the peak conduction velocities identified for the motor nerve were not exactly the same as those for mixed nerve. It may be explained that different nerve fibers belong to the same fiber group (e.g., group A fibers include both motor and sensory fibers) but have different conduction velocity distributions. This is similar to the well reproducible phenomenon that Hoffmann reflex with activation of sensory nerve fibers often has a lower threshold than muscle wave with the activation of motor nerve fibers although both nerve fibers are stimulated by electrical stimulation at the same site (Misiaszek, 2003; Romano and Schieppati, 1987). The overlapping velocity distributions of different components may shift the peaks and make the mixed nerve recording less sensitive for the classification of different components. Another confounding factor is that branching morphogenesis occurs in a single neuron and leads to the relatively thinner and more pruning distal site than the proximal site on the nerve fiber (Lu and Werb, 2008; Menon and Gupton, 2018). As a result, only a portion of nerve fibers might be stimulated by the test stimulus at the distal site although supramaximal intensity was used. The signal could be further contaminated by passage of the descending volley that had the opposite direction to the impulses from distal test stimulation and increased the variations in axonal excitability although our subjects were tested at rest condition. In addition, one technical issue is that the attainment of a full-size test response, which defines the minimum value observed in the velocity distribution, cannot experimentally be reached. This made the identification of the slowest fibers difficult or even impossible. Furthermore, our quadri-pulse technique well defined a distribution of refractory period on the motor nerve bundle with a range of about 0.5–1 ms. The distribution of refractory periods could be more scattered for a mixed nerve with different components. More nerve fibers under subnormal condition during relative refractory period may also explain the complex feature of conduction velocity distribution on a mixed nerve measured with compound nerve action potential (Figure 3A). It should be mentioned that the noninvasive recording used for the compound nerve action potential was preferred in our proof-of-principle study. However, conditioning and test stimuli in the mixed nerve test activated both sensory and motor nerve fibers, producing a significant artifact. As our recording with a bipolar setting was the “waveform subtraction” between the active and reference electrodes, the different amplitudes in two electrodes caused by dispersion of various components (with slow

conduction velocity in particular) might have further reduced our signal-to-noise ratio. It has been demonstrated that a monopolar setting with a near-nerve needle electrode and a remote reference can largely improve the signal-to-noise ratio when compound nerve action potentials are recorded (Eduardo and Burke, 1988). However, the reliability of our recordings was confirmed by the fact that the average of each half of the trials was similar in shape to the full average (Supplementary Figure S2). Noninvasive recordings with a similar monopolar setting using a surface electrode should also be tested in future studies.

4.3. Verification of neuroimaging pipeline

Currently, it is not known how long it takes for nervous impulses to travel between different grey matter regions. Regarding this fundamental question in neuroscience and neurophysiology, novel types of structural and functional data are solicited to probe normal and abnormal brain network functions at the time scale of impulses being transmitted between the nodes in the network. To develop the neuroimaging pipeline with tools and techniques to characterize the latency connectome, we are establishing robust methods to determine the mean or average nerve fiber diameter distribution in the peripheral and central nervous systems. These are being complemented by other works in our group entailing a variety of “microstructure” diffusion weighted magnetic resonance imaging methods obtained with large q-values (Assaf, et al., 2008; Avram, et al., 2016; Basser, et al., 1994; Basser, et al., 2000; Komlosh, et al., 2013). The latency data can potentially be mined for elucidating temporal relationships between different brain networks, providing a window into network functions with normal brain development, particularly the emergence of sensory, motor, language, and their pathways. In addition, the comprehensive brain network characterization and analysis schema will also offer new insights into the causes and mechanisms of developmental delays and dysfunction in disease, degeneration, and trauma. Our proof-of-principle study used a modified version of a classical technique in neurophysiology (Hopf, 1963; Ingram, et al., 1987b). The experiment performed on peripheral nerve fibers within living humans provides ground truth data to inform the neuroimaging framework and is a first step to study a critical problem in neurosciences—measuring the latency connectome. However, a major technical limitation should be mentioned that we set a short distance between two stimuli (about 10 cm) to allow the measurement on a mixed nerve with compound nerve action potential and allow direct comparison of the neurophysiological data with our neuroimaging data (Avram, et al., 2019). As the stimuli with supramaximal intensity spread on the nerve, the short distance between two stimuli may worsen the problem with uncertainty in precise sites of stimuli. Similarly, the inherent limitation of the classical technique with uncertain site of nerve depolarization caused by refractory period, subnormal and supernormal nerve states may also be worsened by short distance between two stimuli. In addition, the interpretation of the collision test may be further complicated by the phase cancellation between the late part of the first compound action potential and the early part of the second potential because two potentials overlap due to short distance between two stimuli. However, the result that amplitudes of test compound muscle action potentials did not change before and after waveform subtraction (Supplementary Figure S1) might suggest that the effect on accuracy of latency measurement with interference of two compound action potentials was minor. Subsequent work will also consider measuring key neurophysiological quantities, such as degree of

myelination, internodal distances, g-ratios, etc. to further inform our neuroimaging experiments and establish correlations between independent measurements obtained from these different quantities. The present study also provided pilot data supporting the possibility of inferring latency measurements for central nervous system. However, more synaptic delays must be taken into account although similar neurophysiological tests can be performed for cortical fibers using noninvasive brain stimulation techniques (Hallett, 2000). In addition, physical properties along the cortical fibers, such as the intra-axonal resistance, membrane resistance and capacitance may be complicated by the highly variable thickness of myelin (Poliak and Peles, 2003) and other astrocyte regulation mechanisms in the brain (Fields, et al., 2015).

5. Conclusion

The collision test with electrical stimulation is a promising technique to measure the conduction velocity distribution of a peripheral nerve. The conduction velocity distributions on motor and mixed nerves are different.

Supplementary Material

Refer to Web version on PubMed Central for supplementary material.

Acknowledgements

This work was done at the National Institutes of Health. This work was supported by BRAIN INITIATIVE Grant #1-R24-MH-109068-01, and the National Institute of Neurological Disorders and Stroke (NINDS) and the *Eunice Kennedy Shriver* National Institute of Child Health and Human Development (NICHD) Intramural Research Programs.

References

Aminoff MJ. Aminoff's Electrodiagnosis in Clinical Neurology. Elsevier; 2012.

Assaf Y, Blumenfeld-Katzir T, Yovel Y, Basser PJ. AxCaliber: a method for measuring axon diameter distribution from diffusion MRI. Magn Reson Med 2008;59:1347–1354. [PubMed: 18506799]

Avram AV, Ni Z, Vial F, Simmons A, Bernstein AS, Leodori G, Pajevic S, Hallett M, et al. The relationship between diffusion MRI-derived axon diameters and conduction velocities in human peripheral nerves. In: International Society for Magnetic Resonance in Medicine, Montreal, Canada, 11–16 5 2019 (Oral Power Pitch).

Avram AV, Sarlls JE, Barnett AS, Ozarslan E, Thomas C, Irfanoglu MO, Hutchinson E, Pierpaoli C, et al. Clinical feasibility of using mean apparent propagator (MAP) MRI to characterize brain tissue microstructure. Neuroimage 2016;127:422–434. [PubMed: 26584864]

Basser PJ, Mattiello J, LeBihan D. MR diffusion tensor spectroscopy and imaging. Biophys J 1994;66:259–267. [PubMed: 8130344]

Basser PJ, Pajevic S, Pierpaoli C, Duda J, Aldroubi A. In vivo fiber tractography using DT-MRI data. Magn Reson Med 2000;44:625–632. [PubMed: 11025519]

Blagburn JM, Bacon JP. Control of central synaptic specificity in insect sensory neurons. Annu Rev Neurosci 2004;27:29–51. [PubMed: 15217325]

Borg J. Axonal refractory period of single short toe extensor motor units in man. J Neurol Neurosurg Psychiatry 1980;43:917–924. [PubMed: 7441271]

Burke RE, Levine DN, Tsairis P, Zajac FE 3rd. Physiological types and histochemical profiles in motor units of the cat gastrocnemius. J Physiol 1973;234:723–748. [PubMed: 4148752]

Burke RE, Tsairis P. Anatomy and innervation ratios in motor units of cat gastrocnemius. J Physiol 1973;234:749–765. [PubMed: 4148753]

Callaghan PT, Coy A, MacGowan D, Packer KJ, Zelaya FO. Diffraction-like effects in NMR diffusion studies of fluids in porous solids. Nature 1991;351:467–469.

Cummins KL, Perkel DH, Dorfman LJ. Nerve fiber conduction-velocity distributions. I. Estimation based on the single-fiber and compound action potentials. Electroencephalogr Clin Neurophysiol 1979;46:634–646. [PubMed: 87308]

Debanne D. Information processing in the axon. Nat Rev Neurosci 2004;5:304–316. [PubMed: 15034555]

Dumitru D. Physiologic basis of potentials recorded in electromyography. Muscle Nerve 2000;23:1667–1685. [PubMed: 11054745]

Eduardo E, Burke D. The optimal recording electrode configuration for compound sensory action potentials. J Neurol Neurosurg Psychiatry 1988;51:684–687. [PubMed: 2841424]

Fields RD, Woo DH, Basser PJ. Glial Regulation of the Neuronal Connectome through Local and Long-Distant Communication. Neuron 2015;86:374–386. [PubMed: 25905811]

Gabriel CM, Howard R, Kinsella N, Lucas S, McColl I, Saldanha G, Hall SM, Hughes RA. Prospective study of the usefulness of sural nerve biopsy. J Neurol Neurosurg Psychiatry 2000;69:442–446. [PubMed: 10990501]

Gesslbauer B, Hruby LA, Roche AD, Farina D, Blumer R, Aszmann OC. Axonal components of nerves innervating the human arm. Ann Neurol 2017;82:396–408. [PubMed: 28833372]

Hallett M. Transcranial magnetic stimulation and the human brain. Nature 2000;406:147–150. [PubMed: 10910346]

Hartline DK, Colman DR. Rapid conduction and the evolution of giant axons and myelinated fibers. Curr Biol 2007;17:R29–35. [PubMed: 17208176]

Hodgkin AL, Huxley AF. Action potentials recorded from inside a nerve fibre. Nature 1939;144:710–711.

Hodgkin AL, Huxley AF. The components of membrane conductance in the giant axon of Loligo. J Physiol 1952;116:473–496. [PubMed: 14946714]

Hopf HC. Electromyographic Study on So-Called Mononeuritis. Arch Neurol 1963;9:307–312. [PubMed: 14049405]

Hursh JB. Conduction velocity and diameter of nerve fibers. Am J Physiol 1939;127:131–139.

Ingram DA, Davis GR, Swash M. The double collision technique: a new method for measurement of the motor nerve refractory period distribution in man. Electroencephalogr Clin Neurophysiol 1987a;66:225–234. [PubMed: 2434306]

Ingram DA, Davis GR, Swash M. Motor nerve conduction velocity distributions in man: results of a new computer-based collision technique. Electroencephalogr Clin Neurophysiol 1987b;66:235–243. [PubMed: 2434307]

Innocenti GM, Caminiti R, Rouiller EM, Knott G, Dyrby TB, Descoteaux M, Thiran JP. Diversity of Cortico-descending Projections: Histological and Diffusion MRI Characterization in the Monkey. Cereb Cortex 2019;29:788–801. [PubMed: 29490005]

Innocenti GM, Vercelli A, Caminiti R. The diameter of cortical axons depends both on the area of origin and target. Cereb Cortex 2014;24:2178–2188. [PubMed: 23529006]

Jacobs JM, Love S. Qualitative and quantitative morphology of human sural nerve at different ages. Brain 1985;108:897–924. [PubMed: 4075078]

King R. Microscopic anatomy: normal structure. Handb Clin Neurol 2013;115:7–27. [PubMed: 23931772]

King R, Ginsberg L. The nerve biopsy: indications, technical aspects, and contribution. Handb Clin Neurol 2013;115:155–170. [PubMed: 23931779]

Komlosh ME, Özarslan E, Lizak MJ, Horkayne-Szakalye I, Freidlin RZ, Horkay F, Basser PJ. Mapping average axon diameters in porcine spinal cord white matter and rat corpus callosum using d-PFG MRI. Neuroimage 2013.

Lu P, Werb Z. Patterning mechanisms of branched organs. Science 2008;322:1506–1509. [PubMed: 19056977]

McGill KC, Lateva ZC. The contribution of the interosseous muscles to the hypothenar compound muscle action potential. Muscle Nerve 1999;22:6–15. [PubMed: 9883852]

Menon S, Gupton S. Recent advances in branching mechanisms underlying neuronal morphogenesis. F1000Res 2018;7.

Misiaszek JE. The H-reflex as a tool in neurophysiology: its limitations and uses in understanding nervous system function. Muscle Nerve 2003;28:144–160. [PubMed: 12872318]

Oh SW, Harris JA, Ng L, Winslow B, Cain N, Mihalas S, Wang Q, Lau C, et al. A mesoscale connectome of the mouse brain. Nature 2014;508:207–214. [PubMed: 24695228]

Olney RK, Budingen HJ, Miller RG. The effect of temporal dispersion on compound action potential area in human peripheral nerve. Muscle Nerve 1987;10:728–733. [PubMed: 3683446]

Padua L, Caliandro P, Stalberg E. A novel approach to the measurement of motor conduction velocity using a single fibre EMG electrode. Clin Neurophysiol 2007;118:1985–1990. [PubMed: 17588808]

Poliak S, Peles E. The local differentiation of myelinated axons at nodes of Ranvier. Nat Rev Neurosci 2003;4:968–980. [PubMed: 14682359]

Ricker K, Hertel G, Stodieck G. Increased voltage of the muscle action potential of normal subjects after local cooling. J Neurol 1977;216:33–38. [PubMed: 72791]

Romano C, Schieppati M. Reflex excitability of human soleus motoneurones during voluntary shortening or lengthening contractions. J Physiol 1987;390:271–284. [PubMed: 3443936]

Schulte-Mattler WJ, Muller T, Georgiadis D, Kornhuber ME, Zierz S. Length dependence of variables associated with temporal dispersion in human motor nerves. Muscle Nerve 2001;24:527–533. [PubMed: 11268025]

Sherman DL, Brophy PJ. Mechanisms of axon ensheathment and myelin growth. Nat Rev Neurosci 2005;6:683–690. [PubMed: 16136172]

Stalberg E. Propagation velocity in human muscle fibres in situ. Acta Physiol Scand (Suppl) 1966;287:1–112. [PubMed: 5958263]

Stalberg E, Trontelj JV. The study of normal and abnormal neuromuscular transmission with single fibre electromyography. J Neurosci Methods 1997;74:145–154. [PubMed: 9219884]

Stalberg E, van Dijk H, Falck B, Kimura J, Neuwirth C, Pitt M, Podnar S, Rubin DI, et al. Standards for quantification of EMG and neurography. Clin Neurophysiol 2019;130:1688–1729. [PubMed: 31213353]

Tankisi H, Burke D, Cui L, de Carvalho M, Kuwabara S, Nandedkar SD, Rutkove S, Stalberg E, et al. Standards of instrumentation of EMG. Clin Neurophysiol 2020;131:243–258. [PubMed: 31761717]

Tasaki I. Nervous transmission. Thomas, Springfield, IL; 1953.

Tomasi S, Caminiti R, Innocenti GM. Areal differences in diameter and length of corticofugal projections. Cereb Cortex 2012;22:1463–1472. [PubMed: 22302056]

van Dijk JG, van Benten I, Kramer CG, Stegeman DF. CMAP amplitude cartography of muscles innervated by the median, ulnar, peroneal, and tibial nerves. Muscle Nerve 1999;22:378–389. [PubMed: 10086899]

Wedeen VJ, Rosene DL, Wang R, Dai G, Mortazavi F, Hagmann P, Kaas JH, Tseng WY. The geometric structure of the brain fiber pathways. Science 2012;335:1628–1634. [PubMed: 22461612]

Highlights

The conduction velocity distribution on a peripheral mixed nerve was measured in living humans. A collision test was performed to measure the conduction velocity distribution of the ulnar nerve. The conduction velocity distributions on a motor nerve and mixed nerve are different.

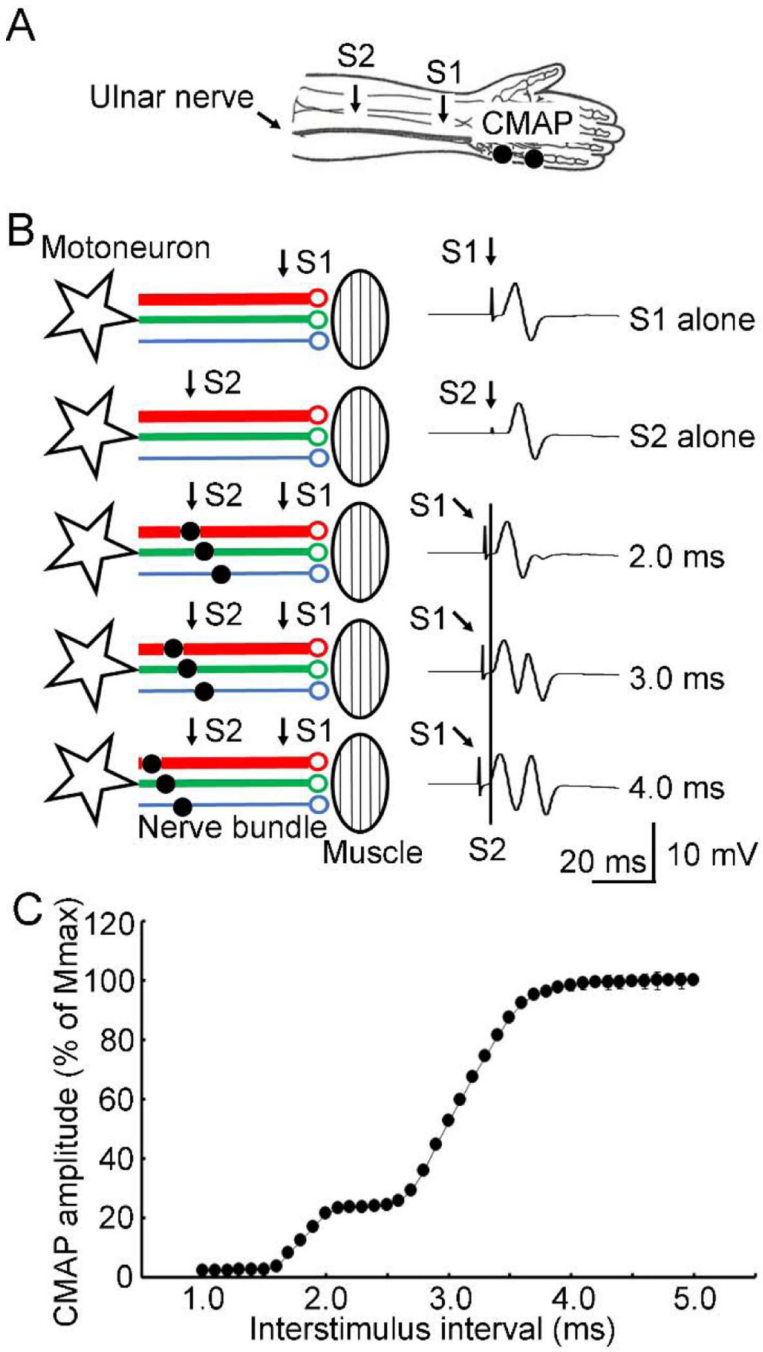

Figure 1. Motor nerve test.

(A) Experimental setup. CMAP was recorded. The ulnar nerve was stimulated with both S1 (conditioning) at the distal and S2 (test) at the proximal sites (labelled with arrows). **(B)** Mechanism and example recordings under different experimental conditions. Stars indicate motoneurons and ellipses indicate muscles. Lines with different colors and thickness indicate nerve fibers with different conduction velocities. Antidromic currents produced by S1 are marked with small black circles on the nerve fibers. S1 was labeled with an arrow and S2 was labeled with a vertical line in the example recordings. Note that progressively

increasing the interstimulus interval allowed the antidromic current to pass the site of S2 on the nerve fibers with faster conduction. This led to the increase in the test (second) CMAP. **(C)** Data analysis for all recordings (mean ± standard deviation) from one subject. Abscissa indicates the interstimulus interval. Ordinate indicates the amplitude of the second (test) CMAP. It was expressed as a percentage value of Mmax. CMAP = compound muscle action potential, Mmax = maximal muscle wave, S1 = first stimulus delivered at distal site, S2 = second stimulus delivered at proximal site.

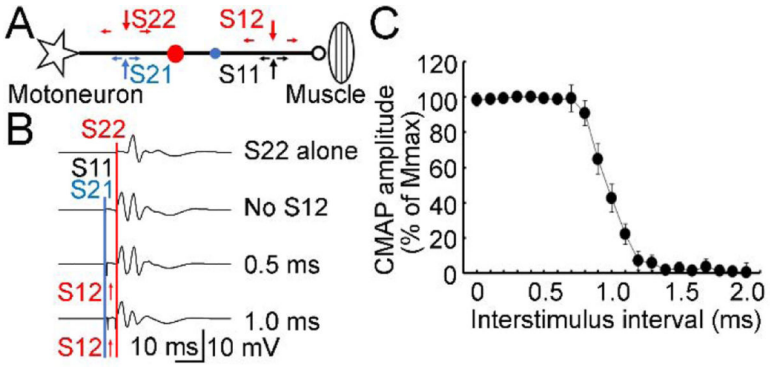

Figure 2. Evaluation of refractory period.

(A) Experimental setup for quadri-pulse technique used to measure the refractory period. CMAP was recorded. Two pulses were delivered both to the distal (S11, black arrows; S12, red arrow) and proximal sites on the ulnar nerve (S21, blue arrow; S22, red arrow). Star indicates a motoneuron and ellipse indicates the muscle. Horizontal small arrows indicate the antidromic and orthodromic currents produced by the stimulations. S11 and S21 were delivered simultaneously and produced the first collision (small blue circle) on the nerve bundle. The antidromic current generated by S12 and the orthodromic current generated by S22 produced the second collision (red circle) on the nerve bundle. **(B)** Example recordings. S22 (red line) was delivered as a test stimulus in all trials. S22 alone at the proximal site (top row) produced the test CMAP with maximal amplitude. The other three rows represented the trials with S22 conditioned by S11 and S21 (blue line, delivered at the same time). An additional CMAP preceding the test CMAP can be recorded (second row with three pulses of S11, S21 and S22). Importantly, a fourth pulse S12 (red arrows) delivered at the distal site between S11 and S22 changed the second (test) CMAP. **(C)** Data analysis for all recordings (mean ± standard deviation) from one subject. Abscissa indicates the interstimulus interval between S11 and S12. Ordinate indicates the amplitude of the second (test) CMAP. It was expressed as a percentage value of Mmax. CMAP = compound muscle action potential, Mmax = maximal muscle wave, S11 = first distal stimulus, S12 = second distal stimulus, S21 = first proximal stimulus, S22 = second proximal stimulus.

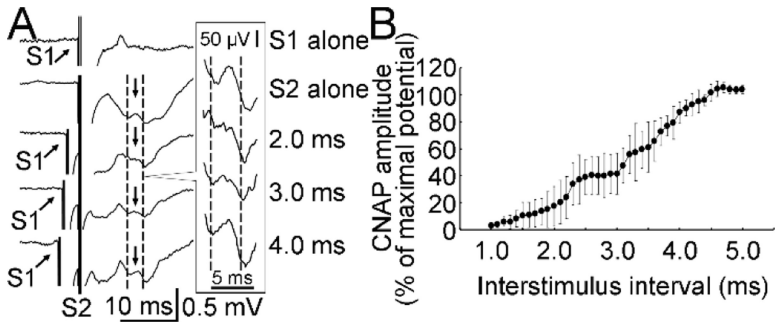

Figure 3. Mixed nerve test.

(A) Example recordings. CNAP on the ulnar nerve was recorded. S1 was labeled with an arrow and S2 was labeled with a vertical line. Two dashed lines and a small arrow between them indicate the test CNAP. The amplitude was measured from the trough to the peak. The test CNAPs between the two dashed lines for the bottom four recordings are shown in a larger scale in the frame on the right side. **(B)** Data analysis for all recordings (mean ± standard deviation) from one subject. Abscissa indicates the interstimulus interval. Ordinate indicates the amplitude of the second (test) CNAP. It was expressed as a percentage value of maximal CNAP with S2 alone. CNAP increased with the increment in interstimulus interval. CNAP = compound nerve action potential, S1 = first stimulus delivered at proximal site, S2 = second stimulus delivered at distal site.

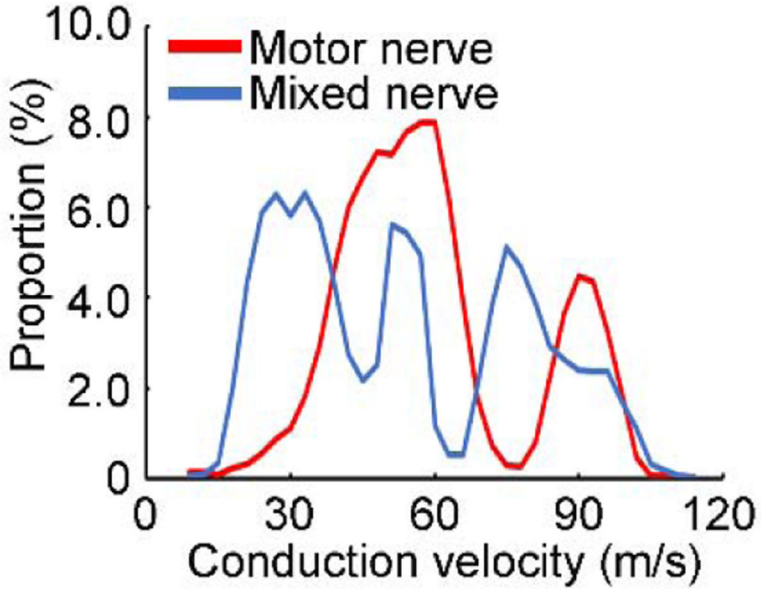

Figure 4. Conduction velocity distributions for motor and mixed nerve fibers.

Data obtained from one subject. Abscissa indicates the conduction velocity of the nerve fiber. Ordinate indicates the proportion (percentage value) of the nerve fibers with certain conduction velocity in the whole bundle. Values on motor and mixed nerve were calculated separately. Red line indicates the distribution of the motor nerve and blue line indicates the distribution of the mixed nerve.

Table 1.

Conduction velocities (m/s) of nerve fibers with different proportions on the motor and mixed nerves

Subject	Motor nerve				Mixed nerve				
	5%	Peak 1	Peak 2	95%	5%	Peak 1	Peak 2	Peak 3	95%
1	27.2	51.6	88.6	103.0	22.9	30.1	51.2	73.8	106.3
2	26.0	51.3	94.0	113.7	17.5	37.7	-	67.0	117.0
3	31.2	48.4	96.6	105.0	24.5	28.0	46.2	67.5	109.6
4	31.8	-	74.5	91.6	23.6	-	41.7	72.2	117.0
5	37.4	52.0	91.2	116.9	26.0	40.0	51.2	84.8	120.0
6	31.8	46.7	89.0	116.8	19.0	32.5	-	87.0	126.6
7	39.1	-	75.6	96.5	21.9	39.9	53.6	73.7	98.2
8	31.9	48.0	88.7	105.3	25.0	45.4	-	87.7	117.6
9	28.7	59.6	100.8	116.2	21.0	-	58.8	85.4	112.0
10	28.7	77.8	108.8	111.6	18.1	26.5	58.6	76.7	114.4
Mean ± SD	31.4 ± 4.2	54.4 ± 10.2	90.8 ± 10.4	107.7 ± 8.9	22.0 ± 3.0	35.0 ± 6.7	51.6 ± 6.2	77.6 ± 8.0	113.9 ± 7.9

Note:

-, Peak was not identifiable